Parallel Sample Processing for Mass Spectrometry-based Single Cell Proteomics

Jing Wang[1], Xue Bo[2], Olanrewaju Awoyemi[1], Herbi Yuliantoro[1], Lihini Tharanga Mendis[1], Amanda DeVor[1], Stephen J. Valentine[1], Peng Li[1]

[1] C. Eugene Bennett Department of Chemistry, West Virginia University, Morgantown, WV
[2] Shared Research Facilities, West Virginia University, Morgantown, WV

* Correspondence should be addressed to P.L. (peng.li@mail.wvu.edu)

Abstract

Background: Single cell mass spectrometry (scMS) has shown great promise for label free proteomics analysis recently. To present single cell samples for proteomics analysis by MS is not a trivial task. Existing methods rely on robotic liquid handlers to scale up sample preparation throughput. The cost associated with specialized equipment hinders the broad adoption of these workflows, and the sequential sample processing nature limits the ultimate throughput.

Results: In this work, we report a parallel sample processing workflow that can simultaneously process 10 single cells without the need of robotic liquid handlers for scMS. This method utilized 3D printed microfluidic devices to form reagent arrays on a glass slide, and a magnetic beads-based streamlined sample processing workflow to present peptides for LC-MS detection. We optimized key operational parameters of the method and demonstrated the quantification consistency among 10 parallel processed samples. Finally, the utility of the method in differentiating cell lines and studying the proteome change induced by drug treatment were demonstrated.

Significance: The present method allows parallel sample processing for single cells without the need of expensive liquid handlers, which has great potential to further improve throughput and decrease the barrier for single cell proteomics.

Introduction

The advent and refinement of single cell RNA sequencing techniques over the past decade has revolutionized our understanding of many physiological and pathological processes at the transcriptome level.[1, 2] Despite the invaluable information revealed by single cell transcriptomics studies, measuring proteomics at the single cell regime cannot be neglected as the level of messenger RNAs and subsequent protein expression is not always correlated. In addition, various post-translation modifications (PTM) to proteins have been shown to have significant impact on their function.[3, 4] However, unlike oligonucleotides, proteins cannot be amplified to facilitate downstream detection, posing significant challenges to measuring proteomics at the single cell level.

Among existing methods for studying single cell proteomics, recent developments in mass

spectrometric analysis of single cells (scMS) have presented the opportunity for analyzing more proteins and PTMs without the need for affinity reagents.[5-7] While early works in scMS were demonstrated in larger cells (e.g., macrophage and mammalian cells),[8-10] recent advancement in sample processing, separation workflow, and data acquisition has enabled scMS for the study of common mammalian cells. To facilitate the widespread adoption of scMS for biological discovery, improvements are still necessary in all facets of scMS, including sample preparation, peptide separation, mass spectrometry detection, data acquisition, and processing.

In scMS, sample preparation is particularly challenging due to the need for minimizing sample loss and excessive sample dilution while maintaining a high throughput measurement. Slavov and co-workers developed effective sample preparation methods for single cell proteomics including minimal Proteomic sample preparation (mPOP) and droplet proteomic sample preparation (nPOP).[11] mPOP employs a freeze-heat cycle to lyse cells and exclusively utilizes chemicals compatible with MS analysis, eliminating the need for sample cleanup. Utilizing an automatic liquid handler system, reagents were added to the 384-well plate to facilitate the freeze-heat cycle for the TMT labeling reaction.[9,12] More recently, by utilizing an acoustic liquid dispensing system and a fluorocarbon-coated glass slide, the nPOP method achieved higher sample preparation throughput and reduced variations among each single cell sample.[13] Kelly and co-workers developed the nanoPOTS (nanodroplet processing in one pot for trace samples) platform.[14-16] The nanoPOTS glass chips featured photolithographically patterned hydrophilic pedestals encircled by a hydrophobic surface, serving as nanodroplet reaction vessels for multi-step proteomic sample processing enabled by a robotic liquid handler.[17] Later, Zhu et al. introduced a nested nanoPOTS (N2) chip, which further improves the single-cell proteomics workflow using isobaric labeling.[18] The N2 chip reduces reaction volumes and can accommodate over 240 single cells on a single microchip. Recently, Kelly and co-workers developed the autoPOTS platform, featuring a fully automated system using a commercial liquid handling robot and autosampler to process and analyze low-input samples efficiently.[19, 20] In addition to liquid handler-based sample preparation workflow, Gebreyesus et al. introduced a microfluidic device named the integrated proteomics chip (iProChip), which was capable of profiling 20 individual mammalian cells simultaneously, providing a streamlined workflow for single-cell sample preparation from cell capture to protein digestion.[21]

Despite the considerable progress in scMS sample preparation, existing methods still rely on robotic nano- to picoliter liquid handlers to achieve high throughput sample preparation. The high cost of adopting these sophisticated units and sequential operation workflow limits the potential of further scaling up sample preparation throughput for scMS. In this work, we report a sample

preparation workflow that does not involve robotic liquid handlers while allowing parallel single cell sample processing (Figure 1a). This method utilized 3D printed channel plates and well plates to form a reagent array on a liquid infused glass surface. Subsequently, a mechanical stage was employed to move a magnet underneath the glass surface to guide magnetic particles moving through reagents in the array to achieve cell lysis and protein capture, reduction, alkylation, digestion, and peptide release. Using this workflow, 10 single cells can be processed simultaneously using a mechanical stage, which can be easily scaled up further due to the low cost of the setup. In this work, we optimized the operational parameters of this workflow and characterized the consistency of the parallel processed samples with TMT labelling experiments. Finally, we demonstrated the feasibility of this setup by measuring the proteome of single H446 and HepG2 cells.

Methods and materials

Chemicals and Reagents

All the solvents used were LC/MS grade. Water, methanol, ethanol, isopropanol, toluene, formic acid, iron filings and concentrated sulfuric acid (98%) were purchased from Fisher Scientific (Hampton, NH, USA). PDMS (polydimethylsiloxane) (Sylgard 184) was obtained from Ellsworth. Silicon wafers (p-type, 100 orientation) were purchased from University Wafers. Dimethyldimethoxysilane was purchased from Tokyo Chemical Industry Co., Ltd. (TCI). Silicone oil and Trypsin (Proteomics Grade) were purchased from Sigma Aldrich (St Louis, MO, USA). Silane PEG (PEG-Si) was purchased from NANOCS, INC. (New York, NY, USA). Sera-Mag beads (Carboxyl Magnetic Beads, hydrophilic) with a diameter of 1 μm were purchased from Fisher Scientific (Hampton, NH, USA). Cell lysis buffer, dithiothreitol (DTT), iodoacetamide, 98%, and TMT10plex™ isobaric label reagents and kits were purchased from Thermo Fisher Scientific (Fair Lawn, NJ, USA).

Device Design and Fabrication

The 3D models of microdevices were designed using SolidWorks 2017 (Waltham, MA, USA), and subsequently exported in STL format. The 3D models were then sliced using Chitubox (Version 1.6). The component part was printed using a Phrozen Sonic Mighty 8K 3D Printer (Taiwan, China). The detailed design of channel plates, well plates and PDMS mold are shown in Figure S1. For the channel plates, the printing material was poly(ethylene glycol) diacrylate (PEGDA) with an average molecular weight of 250. This material was blended with 0.5% (w/w) of Irgacure 819 and 0.5% (w/w) of nitrophenyl phenyl sulfide (NPS). The layer thickness was set at 50 μm, with an exposure time of 20 s per layer and 200 s for the base plate. The printing material for the

PDMS mold and the well plate was Phrozen TR250LV high-temperature resin. Similar to the channel plates, the layer thickness was set at 50 μm, with an exposure time of 2.5 seconds for each layer and 30 seconds for the base plate. Following the printing process, the devices were cleaned with isopropanol, dissolving any unpolymerized material. Subsequently, they underwent a curing process through exposure to UV light for 5 minutes.

Preparation of Surfaces

Preparation of Liquid Infused Surfaces: To prevent the leaching of contaminants from the 3D printing process and to prevent surface sample loss, liquid infused surfaces were prepared on both the 3D printed devices and glass slide. The coating solution was formulated by blending isopropanol, dimethyldimethoxysilane, and sulfuric acid in a volumetric ratio of 100:10:1, as reported in our prior works.[22,23] The solution was gently agitated for approximately 30 seconds and left to stand at room temperature for 30 min. To coat the glass slide, a NO.2 glass slide was immersed in the coating solution for a duration of 10 seconds and then left to air dry overnight at room temperature. To create a stable lubricant surface, 50 μL of silicone oil was introduced onto the glass slide and evenly spread by air dispersion. To coat the 3D printing devices, the surfaces were initially treated using a Plasma Cleaner (Harrick Plasma) to expose free radicals on the surface. Subsequently, the coating solution was introduced into the channel for 10 seconds and left to air dry at room temperature for 2 hours. Following this, 20 μL of silicone oil was introduced into the device to facilitate the formation of a stable lubricant layer. The entire channel was then rinsed with isopropanol to remove any excess silicone oil and dried using ambient air.

Formation of Silane-PEG array on the glass slide: To create the Silane-PEG array, mPEG-silane (Biopharma PEG Scientific Inc) with a molecular weight of ~5k was initially dissolved in an ethanol/water solution with a volumetric ratio of 95:5 at a concentration of 15 mg/mL. This solution was then brought into contact with the modified glass slide and maintained at 65°C for a minimum of 2 hours. Under these conditions, mPEG-silane forms covalent bonds with the material, ensuring a robust and enduring attachment. To create microarrays on the glass slide, a PDMS mold with a configuration of 6x10 holes was used for delivering the silane PEG solution to the glass slide. Following the application of the silane solution, the PDMS mold and the modified glass slide combination were incubated overnight in an oven at 65°C. This process was carried out to achieve the desired PEG coating atop the liquid-infused glass slide. The schematic of the coating step is shown in Figure S2.

Surface modification for 3D Printed molds: To ensure proper curing of PDMS, the 3D printed molds were modified using PDMS prepolymers, carbonyl iron particles (CIPs), and toluene in a

weight ratio of 2:3:5.[24] To ensure a uniform mixture, the component containing CIPs underwent vigorous stirring for 20 minutes. Subsequently, this solution was sprayed onto the 3D printed mold using an airbrush. Following this step, a mixture of PDMS prepolymers and curing agent in a 10:1 ratio was poured onto the 3D printed mold. The curing process was then carried out for 1 hour at a temperature of 65°C, resulting in the complete curing of PDMS on the 3D printed mold.

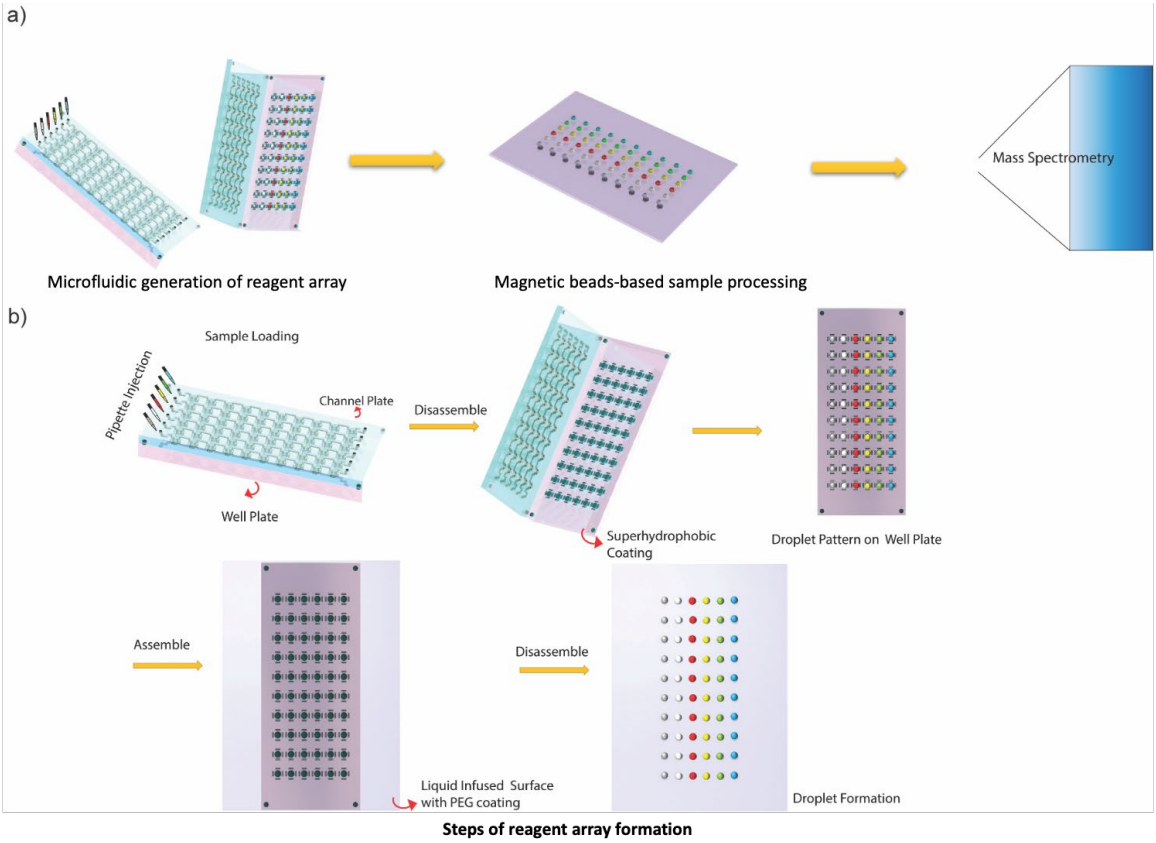

Figure 1. a) Schematic of the whole workflow for the nanodroplet processing system. b) Detailed steps for generating the reagent array on a glass slide

Superhydrophobic coating for the channel plates and well plates: The outer surfaces of the channel plates and well plates were modified with superhydrophobic coating, Ultra-Ever Dry, which was used in our previous works.[25,26] To achieve a uniform coating of the device surfaces, we employed an air-powered sprayer to apply two layers of the coating reagent. To prevent inadvertent superhydrophobic coating on the inner surfaces of the wells, we employed 3D printed shield modules. These modules were designed to fit with the well plates, effectively shielding the wells from the coating spray. The lower coating layer was allowed to dry for 30 minutes, while the upper coating layer was allowed to cure for 2 hours. Following the curing process, all the devices underwent a thorough washing with water and were subsequently dried with a flow of air.

Nanoflow LC−MS/MS Analysis

For nanoLC-MS analysis, a flow rate of 200 nL/min was employed, utilizing an Easy-Spray™ PepMap™ Neo column (particle size: 2 μm, diameter: 75 μm, length: 150 mm) from Thermo Fisher Scientific. Here, Ultimate 3000 RSLC nano (Thermo Fisher Scientific) was employed to run all the samples. It should be noted that the autosampler of the nanoLC systems requires a sample volume of ~20 μL for stable sample pickup due to technical issues. The mobile phases consisted of water with 0.1% formic acid (buffer A) and acetonitrile with 0.1% formic acid (buffer B). A linear gradient spanning 180 min with the equilibration of 2% buffer B for 5 minutes, transitioning from 8% to 30% buffer B, was employed for the LC separation. Subsequently, the LC column underwent a washing step, with buffer B ramped to 45% over 15 minutes and further increased to 90% in 5 minutes. Finally, re-equilibration was achieved with 2% buffer B for an additional 10 minutes.

A Q-Exactive hybrid quadrupole Orbitrap mass spectrometer (Thermo Fisher Scientific) was employed for all data acquisition under data dependent acquisition mode. The separated peptides were ionized at a spray voltage of 2.5 kV, and the resulting ions were directed into an ion transfer capillary maintained at 250°C. The voltage of S-lens was set to 50 V. For MS1 scans, a mass range of 275 to 1800 was employed, with a scan resolution of 140,000, an AGC target of 1×10^6, and a maximum injection time of 50 ms. MS/MS scans were executed with an AGC target of 1×10^5, at a resolution of 17,500, and a maximum injection time of 50 ms. The 10 most abundant precursor ions in each full MS1 spectrum were selected for fragmentation. The fixed first mass of 50.0 m/z with the isolation window of 1.6 *m/z* was used for fragmentation with a normalized collision energy of 28.

Generation of droplet array

The process for generating droplet reagent arrays involves 2 steps: 1) assembling the channel plate and well plate, loading reagents through distinct inlets; 2) combining the well plate with the liquid-infused glass surface coated with PEG (Figure 1b). The results of droplet generation on the glass slide rely on the leak-proof assembly of the well and channel plates, and the PEG coating. To ensure uniform transfer of reagent arrays onto the well plate, it is crucial that the assembly of the well plate and glass slide maintains consistent contact across the same surface with equal force.

Proteomic Sample Preparation

Upon achieving the reagent array on the glass slide, the magnetic beads were moved to the sample droplet for protein extraction using a mechanical stage. This extraction process was conducted at room temperature for 3 minutes. Subsequently, a mechanical stage guided the

movement of the magnet beneath the glass slide, directing the movement of magnetic beads through consecutive droplets containing 0.2% DDM (Dodecyl-β-D-maltoside) and 5 mM TCEP (Tris(2-carboxyethyl) phosphine) in 100 mM TEAB (Triethylammonium bicarbonate), and 30 mM IAA (Iodoacetamide) in 100 mM TEAB. After each movement, the magnets were slightly moved around to allow good dispersion of the beads, and the beads were then incubated for 15 min for reduction and alkylation, respectively. Finally, the magnetic beads were moved to the trypsin digestion solution, incubating for 3 hours at 37 °C. Throughout the preparation steps, no special humidity control was employed, and the droplets were allowed to dry after incubation.

In the TMT quantification experiment, post-enzyme digestion, the digested peptide samples were directed to the TMT labeling reagents. Each reagent, containing 0.8 mg in 41 μL of acetonitrile, was utilized for labeling. Following a 45-minute TMT labeling reaction, all the released peptide samples would be gathered using a 0.1% formic acid solution for subsequent nano LC-MS analysis.

For the label-free quantification experiment, individual samples were collected one by one using a 0.1% formic acid solution. These prepared samples were then made ready for nanoLC-MS analysis.

Cell culture

Two cell lines (small cell lung cancer cell line H446 and HepG2) were obtained from ATCC. HepG2 cells were cultured at 37°C with 5% CO_2 in Dulbecco's Modified Eagle's Medium (DMEM) obtained from Corning in Arizona, USA. The growth medium was supplemented with 10% fetal bovine serum and 1× penicillin-streptomycin, also sourced from Corning in Arizona, USA. H446 cells were cultured in RPMI 1640 medium, which included L-glutamine and was without glucose, obtained from Corning. The RPMI 1640 medium was supplemented with 10% fetal bovine serum and 1× penicillin-streptomycin. For drug treatment experiments, H446 cells sample were treated with 2 μM doxycycline after reaching a confluence level of 70-80%.

Data Analysis

The identification and quantification of peptides and proteins were conducted using MaxQuant software (version 2.1.4.0). Two different databases were used for the cytochrome c and myoglobin mixtures: the human UniProt KB database (fasta file 9606, downloaded on January 15, 2023, containing 208,022 sequences) and the horse UniProt KB database (fasta file 9796, downloaded on January 15, 2023, containing 75,451 sequences). For all other cell experiments, the human UniProt KB database (fasta file 9606, downloaded on January 15, 2023, containing 20,198 sequences) was employed. The following search parameters were applied: a precursor mass

tolerance of 20 ppm and a fragment ion mass tolerance of 0.1 Da. Trypsin was specified as the enzyme with a maximum allowance of 2 missed cleavages. Fixed modifications included cysteine carbamidomethylation, while variable modifications encompassed oxidation of methionine and deamidation of asparagine and glutamine. In the case of label-free quantification (LFQ) for H446 and HepG2 cell samples, Match Between Runs (MBR) was activated with a matching window of 0.4 min and an alignment window of 10 min. LFQ calculations were conducted separately within each parameter group containing the single cell loading. Both unique and razor peptides were chosen for protein quantification. All other unspecified parameters remained at the default settings of MaxQuant software. LFQ intensities were extracted and filtered to include values with a validity of at least 70. For TMT-based quantification, corrected reporter ion intensities were extracted. To mitigate batch effects arising from multiple TMT experiments, relative abundances from 10-plex TMT were subjected to a (log2)-transformation. Following this transformation, the data were subjected to additional processing and visualization using OriginLab 2020. To be considered as "quantifiable," proteins needed to meet specific criteria, including having more than 70% valid values and at least two identified peptides per protein. The MS proteomics data have been deposited to the ProteomeXchange Consortium via the PRIDE partner repository with the dataset identifier PXD04898 (For review, Username: reviewer_pxd048984@ebi.ac.uk; Password: 5DmQr0Wg).

Results and Discussion

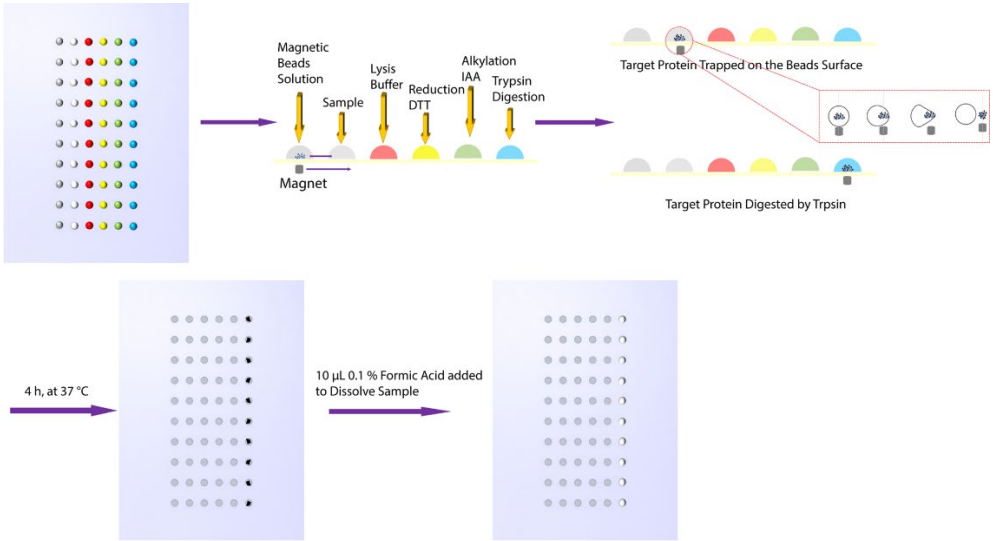

Figure 2. Schematic of magnetic beads-based sample preparation workflow.

System Design and Operation

The goal of the workflow is to achieve scalable single cell preparation without the need for a robotic high precision liquid handling system. The overall workflow is comprised of two parts: 1) rapid formation of reagents arrays; 2) magnetic beads-based cell lysis and peptide digestion for parallel sample processing. The first part was achieved based on a composable 3D printed microfluidic plates (cPlate) fluid manipulation scheme reported by our group recently.[26] As shown in Figure 1b, the cPlate fluid manipulation involves the assembly of a microwell plate and a microchannel plate so that reagents can be loaded into each well using a pipette. After disassembly of the two plates, reagents in each well were transferred onto the surface of a glass slide via contact transfer, forming a reagent array on the slide (Figure S3, Supporting Information). To minimize sample adsorption and facilitate the contact transfer, the glass slide was pre-coated with a mPEG-Silane spot array that aligns with microwells. As proof of concept, the reagent array is designed to be 6x10, allowing simultaneous processing of 10 cells with 6 different reagents. The final reagent droplet volume is approximately 1.75 μL, resulting in a contact area of <0.8 mm^2.

After the reagent array was formed, we adapted a magnetic beads-based workflow to prepare peptides for LC-MS analysis. As shown in Figure 2, the magnetic beads were first mixed with the cell droplet by moving magnets, and the single cell was trapped by the overwhelming magnetic beads and transported to the lysis droplets. After cell lysis, proteins were captured by the magnetic beads and transported to the reduction and alkylation droplets, and finally the trypsin digestion droplets (Video S1, Supporting Information). Digestion was allowed for 180 min at 37 ℃ until the droplets dried. Finally, peptides were released from the magnetic beads using 0.1% formic acid solution, which is ready for LC-MS analysis.

Optimization of operational parameters for the sample preparation workflow

We first optimized the volume of reagent droplets using 0.2 ng mixture of myoglobin and cytochrome C. The volume of reagent droplets can be controlled by the dimension of microwells. We examined 4 volumes, including 500 nL, 1 μL, 1.75 μL, and 10 μL, while keeping the total protein amount at 0.2 ng. All the samples were processed through the magnetic beads-based workflow, and digested peptides were analyzed using nanoLC-MS. We used sequence coverage as the metric to compare different reagent volumes, which minimizes the influence of the signal variations caused by the ionization source and instrument. It should be noted that for conditions with similar protein coverage slight differences in performance may still exist and require further studies. As shown in Figure 3a, reagent droplets with volumes of 1 μL and 1.75 μL achieved the highest coverage for both myoglobin and cytochrome c. As the reagent volume increased to 10 μL, we observed a significant drop in sequence coverage for both proteins. For the following

studies, we chose 1.75 µL as the optimal reagent volume, which corresponds to a radius of 1 mm microwell.

Another important factor that affects the sample preparation results is the amount of magnetic beads. For low sample amounts, it is necessary to have large amounts of beads to ensure high capture rates of proteins. We tested 3 bead amounts, 25, 50, and 100 µg. Figure 3b showed that the sequence coverage with 25 µg beads was significantly lower than the groups with 50 and 100 µg beads. The larger amount of magnetic beads increases the overall surface capture area and decrease the diffusion distance for proteins, which may explain the improved the coverage with more magnetic beads. Since sequence coverage for the 50 and 100 µg samples is the same, we chose the 50 µg bead amount for the following analysis to reduce the reagent consumption.

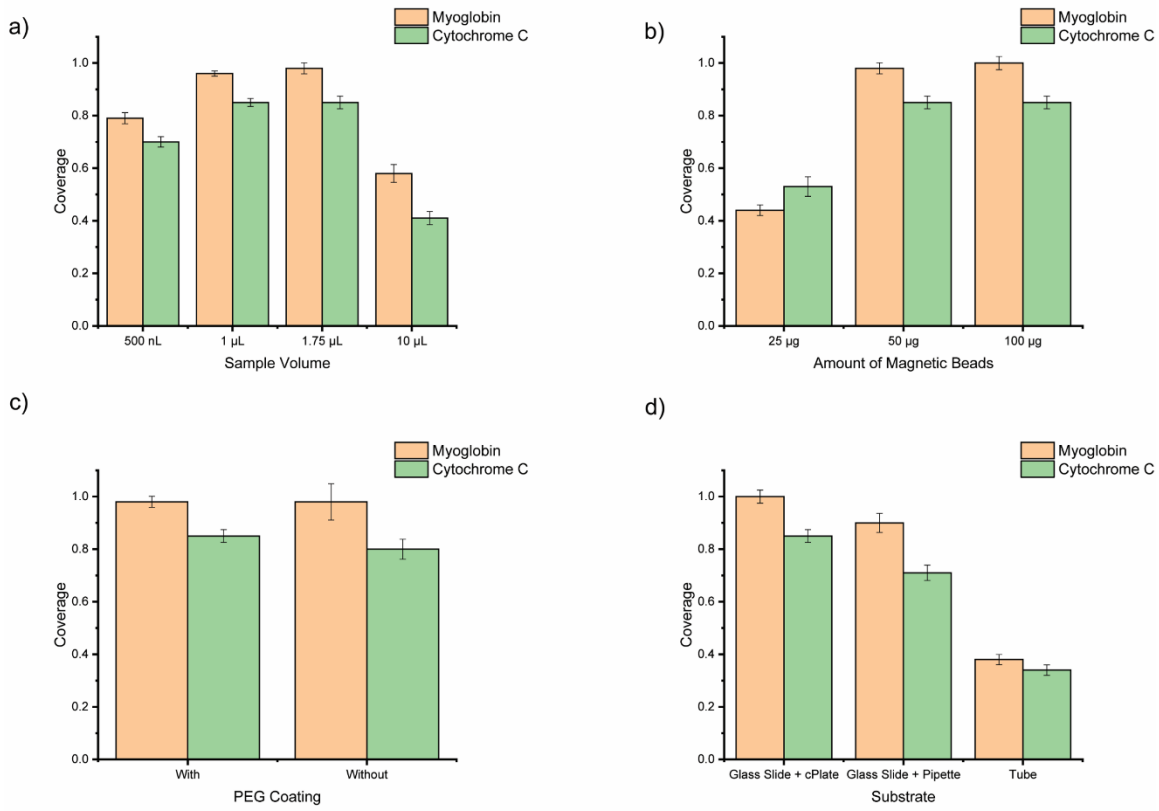

Figure 3. Comparison of peptide coverage of 0.2 ng mixture of myoglobin and cytochrome C under different reagent volumes (a), amount of magnetic beads (b), PEG coating (c), and types of sample preparation workflows (d).

Additionally, to facilitate the transfer of droplets from microwell plates onto the liquid infused surface, we fabricated a hydrophilic spot array on the glass slide. To avoid excessive sample loss on the hydrophilic spot, we used methoxy silane functionalized polyethylene glycol (silane PEG)

coating which can suppress the non-specific binding of proteins to the surface. We examined the impact of the silane PEG coating in the sample preparation results using 0.2 ng myoglobin and cytochrome c. When there is no hydrophilic spot on the liquid infused surface, droplets cannot be transferred onto the surface using the microwell plate. Therefore, we manually created a droplet array using a pipette for comparison. All other sample preparation steps were the same for the two groups. As shown in Figure 3c, no significant difference in sequence coverage was observed between the methoxyl silane functionalized polyethylene glycol coated group and the liquid infused surface only group, indicating the feasibility of using silane PEG coating for enabling the parallel transfer of reagent droplets onto the liquid infused surface.

Finally, we compared the performance of the present parallel sample preparation workflow with two alternative protocols using sequential reagent loading. The first alternative protocol was to manually perform all reagent addition steps using a pipette on the same glass slide as the magnetic beads-based parallel workflow. The second alternative protocol was to perform all reagent addition steps manually using a pipette in a microcentrifuge tube. Again, we used 0.2 ng myoglobin and cytochrome c to evaluate the sequence coverage after these protocols. Figure 3d showed the parallel workflow achieved the best coverage for both proteins among the 3 protocols. While the manual pipette reagent loading on the glass surface protocol achieved slightly less sequence coverage than the magnetic beads protocol, it is much more time and labor consuming than the parallel workflow.

Quantification consistency among parallel processed samples

One potential concern of using one-step reagent droplet transfer is the variation in reagent volumes which may affect the quantification reliability among different samples. Here, we tested the consistency of the droplets using fluorescence measurement and mass spectrometry detection. First, we loaded fluorescent solution into microwells and transferred the solution onto a glass slide to form a fluorescent droplet array. Figure 4a shows 30 droplets each with a volume of 1.75 μL transferred onto the glass slide, and we measured the fluorescence intensity using an imaging system (ChemiDoc MP imager, Bio-Rad). Across the 30 droplets measured, a CV of 4.8% was achieved, indicating a good consistency in the droplet amount after transferring.

In addition, we examined the quantification consistency among droplets using MS detection. Here, we employed tandem mass tag (TMT)-based quantification of 0.2 ng mixture of myoglobin and cytochrome *c*. 10 identical samples were processed with the parallel workflow including reduction, alkylation, trypsin digestion, TMT labeling, and quenching. For all 10 samples, the median values of log2-transformed protein intensities for myoglobin ranged from 12 to 12.5, while for cytochrome

c, the log2-transformed median intensity was between 9.2 and 9.7 (Figure 4b). Pair-wise analysis of the single-cell-equivalent TMT channels revealed Pearson's correlation coefficients ranging from 0.92 to 1 across the 10 samples (Figure 4c and 4d). These results support the reliability of using the parallel workflow for quantitative analysis using MS.

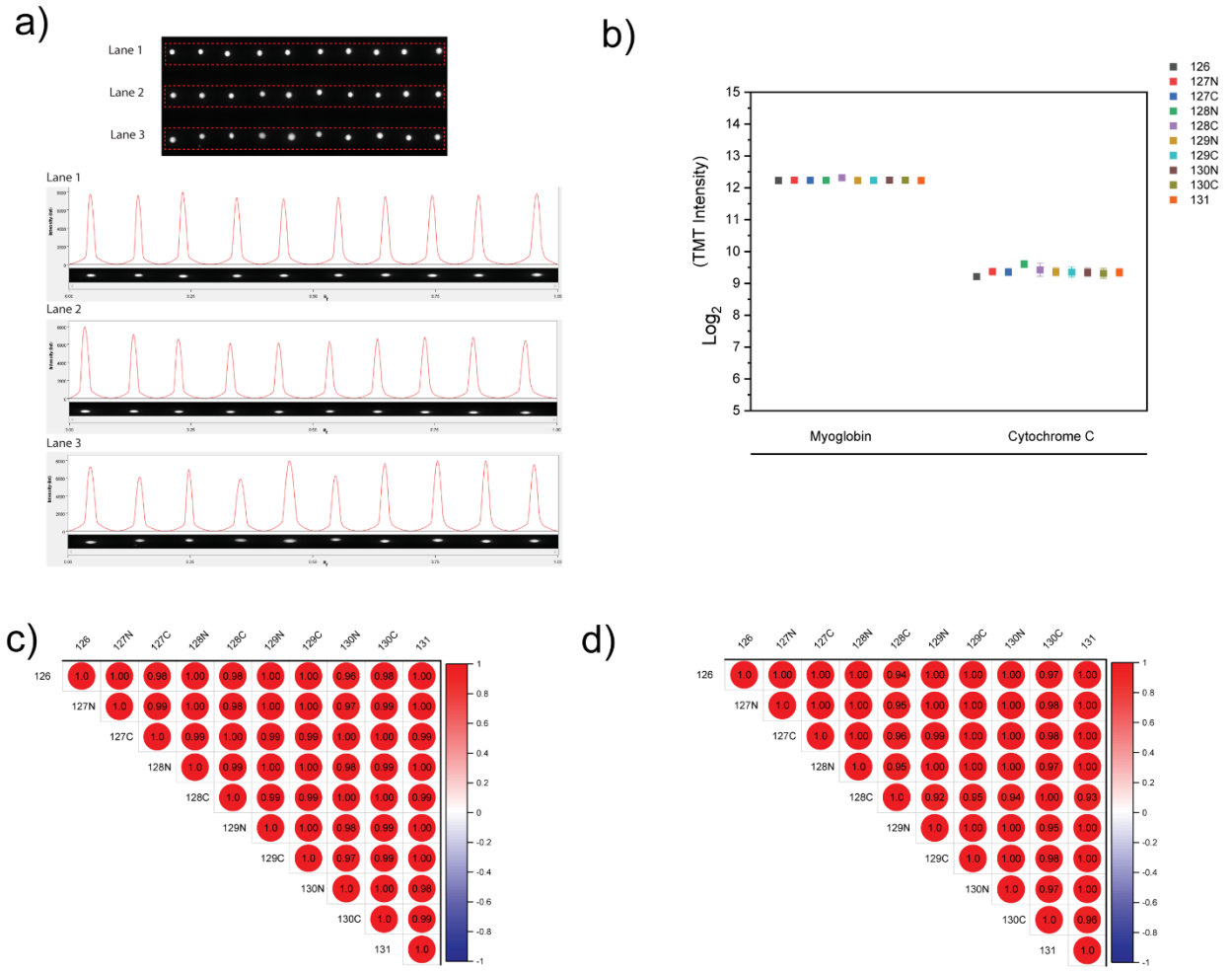

Figure 4. Evaluation of quantification consistency amount for 10 parallel samples. a) Images and fluorescence intensity of 30 droplets containing fluorescein. b) Distribution of protein intensities for myoglobin and cytochrome c across 10 TMT channels processed simultaneously. The error bars represent the entire range of the CV for the total amount of quantified proteins by TMT. c) Pairwise correlation of protein intensities across the 10 samples for myoglobin. d) Pairwise correlation of protein intensities across the 10 samples for cytochrome c.

Application to single cell proteomics

Finally, we performed single cell proteomics analysis using the parallel workflow. While single cells were picked manually under a microscope for this study, the open platform of the present allows it to be interfaced with a cell sorter in future studies. We evaluated the performance of the

present sample preparation workflow using the human small cell lung cancer cell line (H446) and human liver cancer cell line (HepG2). Under the criteria of an FDR cutoff of <0.01 and without MS1-level feature matching (as depicted in Figure 5), an average of 569 protein groups were identified from single H446 cells, while 360 protein groups were identified from HepG2 cells. The results of 4 independent experiments with H446 cells displayed a 60% overlap in the identified protein groups. Proteins identified with one H446 cell are listed in Table S1. As a control experiment, we also performed 0 cell analysis to assess the influence of cell culture medium and the overall workflow on protein identification. For the 0-cell sample, we identified ~49 proteins, indicating that the majority of proteins identified in our single cell analysis were indeed from single cells. Admittedly, the number of proteins identified in single cells here are less compared with state-of-the-art reports. While the sample preparation step is critical in single cell proteomics, the proteins identified are also influenced by the nanoLC-MS process. In this study, we used a standard nanoLC-MS system with a commercial column (Ultimate 3000 nanoLC, PepMap™ Neo columns, and a Thermo Fisher Q-exactive mass spectrometer). In addition, due to technical issues, the autosampler of the nanoLC required ~20 μL for reliable sample pickup, which adversely affected the nanoLC-MS results. To better evaluate the potential of the present sample preparation workflow, we measured the proteome of 10 and ~1000 H446 cells using the same nanoLC-MS system, which identified ~950 and ~1460 proteins, respectively (Figure S4). As a comparison, Zhu et al. detected ~675 proteins in a single HeLa cell and >6000 proteins in ~650 HeLa cells. Gebreyesus et al. identified ~1000 proteins in single cell samples and >6000 proteins in ~6000 cells samples. The percentage of proteins identified in single cells samples to bulk samples for the present method is ~30%, whereas the literature values are ~10-20%. This comparison indicates the potential for further performance improvement of the present method when combined with the state-of-the-art nanoLC and mass spectrometers and improved data acquisition methods. We also compared the results obtained using the present protocol and a manual pipette protocol. 357+/-28 proteins were identified with the present protocol, whereas 292+/-23 proteins were identified with pipette protocol (Figure S5). The present protocol showed ~20% improvement in terms of the number of proteins identified.

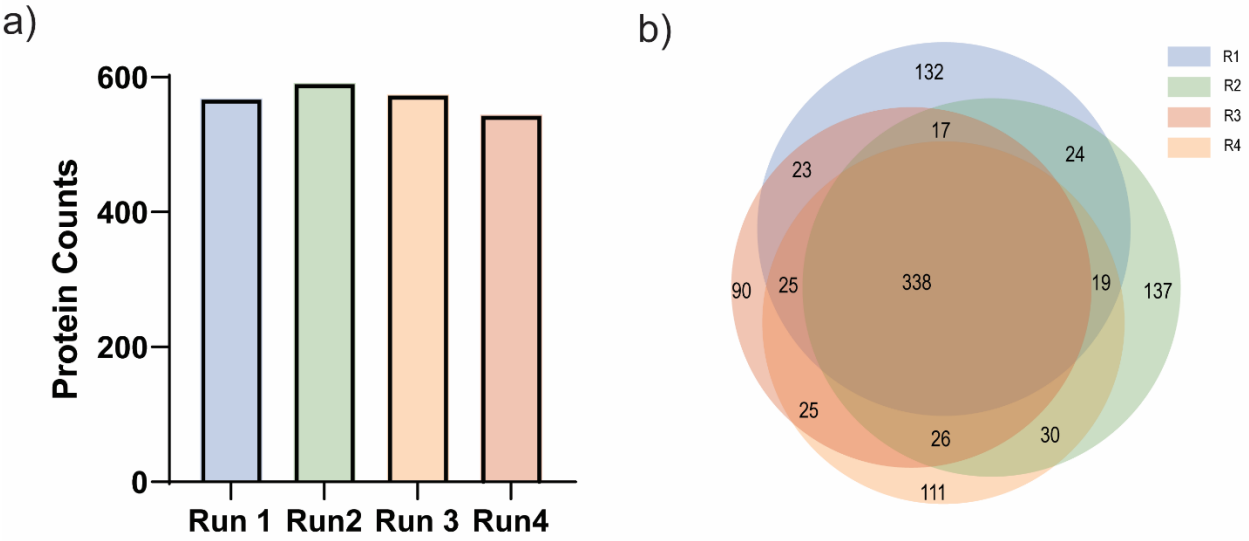

Figure 5. a) Unique protein groups identified from 4 single H446 cells. b) Venn diagrams showing the overlap of protein identifications in 4 single H446 cells.

As a proof-of-concept, we examined the utility of this method for differentiating different cell lines. Figure 6a shows the effective differentiation of 5 single H446 cells and 5 single HepG2 cells by principal component analysis (PCA), as they clustered distinctively by cell type. Here, normalization was performed using the 'Precursor Ions Quantifier' feature within Proteome Discover. The normalization was set to 'total peptide amount' mode, while keeping all other parameters at their default settings. The PCA plot accounts for 351 protein features, indicating distinct proteomic profiles between HepG2 and H446 cells with 41% variation. This result demonstrated the potential of the present sample preparation workflow through clear differentiation between these two cell populations.

We also studied the impact of doxycycline treatment on the proteomes of H466 human lung cancer cells. We applied a 2 μM doxycycline treatment to H446 cells for 24 hours. Subsequently, one treated H446 cell and one untreated H446 cell were selected for analysis using the parallel workflow. The results revealed that among the 329 quantifiable protein groups, 28 displayed significant differential abundance in the treated H446 cell relative to the untreated control H446 cell ($p < 0.05$, $|\text{fold difference}| \geqslant 2$) (Figure 6b).

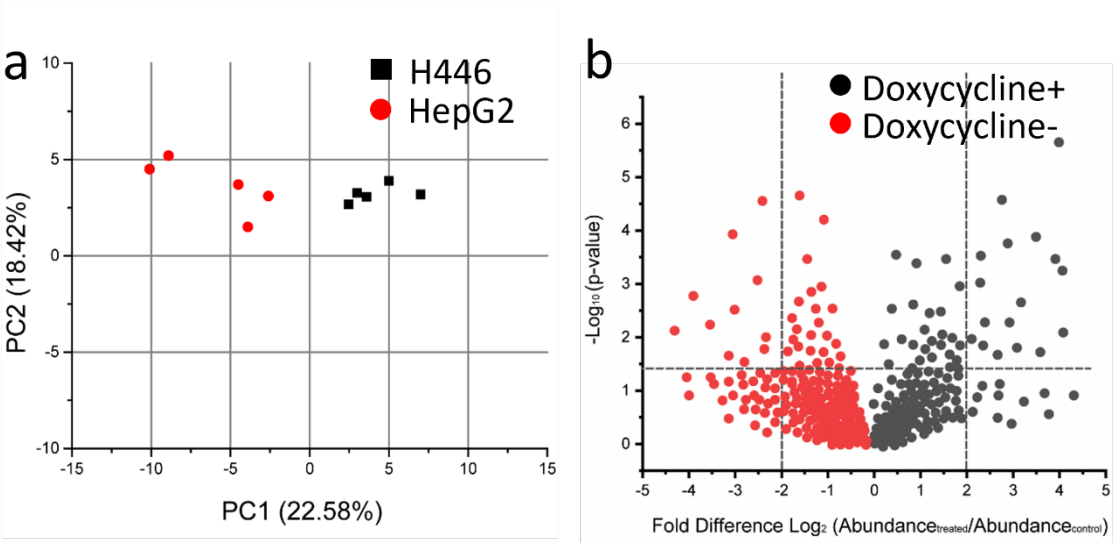

Figure 6. a) PCA of 5 single H446 cells and 5 single HepG2 cells with 351 protein features. b) Volcano plot indicating significant differences in protein expression for quantifiable protein groups ($p < 0.05$, $|\text{fold difference}| \geq 2$) between tween H446 cells.

Conclusion

In this current study, we present a novel sample preparation workflow that avoids the need for robotic liquid handlers. By employing a 3D printed channel plate, a well plate, and a liquid-infused glass surface, a reagent array can be generated to facilitate cell lysis and subsequent proteomic sample processing. A mechanical stage guides magnetic particles through the reagent array, achieving cell lysis, protein capture, reduction, alkylation, digestion, and peptide release. Notably, this workflow allows for the parallel processing of ten single cells using a mechanical stage, with the potential for further scalability due to its cost-effectiveness. The optimization and characterization of this workflow have been demonstrated, along with its applicability in measuring the proteome of single cells. This work introduces a new concept of streamlining sample processing workflow for single cell proteomics. Compared with existing liquid robotics-based methods with single reagent dispensing step, the present workflow still needs to further improve its overall throughput to meet the needs of single cell studies. Improvement in the integration mechanical stage operation and the plate transfer and the efficiency of droplet arrangement will unlock the potential of the methods for large scale studies.

Acknowledgement

We acknowledge the partial support of this work from National Institute of Health R01GM135432 and National Science Foundation ECCS-2144216. We acknowledge the use of WVU shared research facilities.

Supporting Information

Detailed design of 3D printed devices, workflow for surface modification, and images showing the formation of reagent array are available in the supporting information (PDF). A video showing the movement of magnetic particles on the surface is also included (MP4).

References

1. Hwang, B.; Lee, J. H.; Bang, D., Single-cell RNA sequencing technologies and bioinformaticspipelines. *Experimental & Molecular Medicine* **2018,** *50* (8), 1-14.
2. Jovic, D.; Liang, X.; Zeng, H.; Lin, L.; Xu, F.; Luo, Y., Single-cell RNA sequencing technologies and applications: A brief overview. *Clinical and Translational Medicine* **2022,** *12* (3), e694.
3. Bond, A. E.; Row, P. E.; Dudley, E., Post-translation modification of proteins; methodologies and applications in plant sciences. *Phytochemistry* **2011,** *72* (10), 975-996.
4. Shi, X.-X.; Wang, Z.-Z.; Wang, Y.-L.; Huang, G.-Y.; Yang, J.-F.; Wang, F.; Hao, G.-F.; Yang, G.-F., PTMdyna: exploring the influence of post-translation modifications on protein conformational dynamics. *Briefings in Bioinformatics* **2021,** *23* (1).
5. Mann, M.; Jensen, O. N., Proteomic analysis of post-translational modifications. *Nature Biotechnology* **2003,** *21* (3), 255-261.
6. Nørregaard Jensen, O., Modification-specific proteomics: characterization of post-translational modifications by mass spectrometry. *Current Opinion in Chemical Biology* **2004,** *8* (1), 33-41.
7. Orsburn, B. C.; Yuan, Y.; Bumpus, N. N., Insights into protein post-translational modification landscapes of individual human cells by trapped ion mobility time-of-flight mass spectrometry. *Nature Communications* **2022,** *13* (1), 7246.
8. Félix, I.; Jokela, H.; Karhula, J.; Kotaja, N.; Savontaus, E.; Salmi, M.; Rantakari, P., Single-Cell Proteomics Reveals the Defined Heterogeneity of Resident Macrophages in White Adipose Tissue. **2021,** *12*.
9. Specht, H.; Emmott, E.; Petelski, A. A.; Huffman, R. G.; Perlman, D. H.; Serra, M.; Kharchenko, P.; Koller, A.; Slavov, N., Single-cell proteomic and transcriptomic analysis of macrophage heterogeneity using SCoPE2. *Genome Biology* **2021,** *22* (1), 50.
10. Cong, Y.; Motamedchaboki, K.; Misal, S. A.; Liang, Y.; Guise, A. J.; Truong, T.; Huguet, R.; Plowey, E. D.; Zhu, Y.; Lopez-Ferrer, D.; Kelly, R. T., Ultrasensitive single-cell proteomics workflow identifies >1000 protein groups per mammalian cell. *Chemical Science* **2021,** *12* (3), 1001-1006.
11. Slavov, N., Driving Single Cell Proteomics Forward with Innovation. *Journal of Proteome Research* **2021,** *20* (11), 4915-4918.
12. Petelski, A. A.; Emmott, E.; Leduc, A.; Huffman, R. G.; Specht, H.; Perlman, D. H.; Slavov, N., Multiplexed single-cell proteomics using SCoPE2. *Nature Protocols* **2021,** *16* (12), 5398-5425.
13. Leduc, A.; Huffman, R. G.; Cantlon, J.; Khan, S.; Slavov, N., Exploring functional protein covariation across single cells using nPOP. *Genome Biology* **2022,** *23* (1), 261.
14. Pace, C. L.; Simmons, J.; Kelly, R. T.; Muddiman, D. C., Multimodal Mass Spectrometry Imaging of Rat Brain Using IR-MALDESI and NanoPOTS-LC-MS/MS. *Journal of Proteome Research* **2022,** *21* (3), 713-720.
15. Kelly, R.; Zhu, Y.; Liang, Y.; Cong, Y.; Piehowski, P.; Dou, M.; Zhao, R.; Qian, W. J.; Burnum-Johnson, K.; Ansong, C., *Single Cell Proteome Mapping of Tissue Heterogeneity Using Microfluidic Nanodroplet Sample Processing and Ultrasensitive LC-MS*. J Biomol Tech. 2019 Dec;30(Suppl):S61.: 2019.
16. Williams, S. M.; Liyu, A. V.; Tsai, C.-F.; Moore, R. J.; Orton, D. J.; Chrisler, W. B.; Gaffrey, M. J.; Liu, T.; Smith, R. D.; Kelly, R. T.; Pasa-Tolic, L.; Zhu, Y., Automated Coupling of Nanodroplet Sample Preparation with Liquid Chromatography–Mass Spectrometry for High-

Throughput Single-Cell Proteomics. *Analytical Chemistry* **2020,** *92* (15), 10588-10596.
17. Zhu, Y.; Piehowski, P. D.; Zhao, R.; Chen, J.; Shen, Y.; Moore, R. J.; Shukla, A. K.; Petyuk, V. A.; Campbell-Thompson, M.; Mathews, C. E.; Smith, R. D.; Qian, W.-J.; Kelly, R. T., Nanodroplet processing platform for deep and quantitative proteome profiling of 10–100 mammalian cells. *Nature Communications* **2018,** *9* (1), 882.
18. Woo, J.; Williams, S. M.; Markillie, L. M.; Feng, S.; Tsai, C.-F.; Aguilera-Vazquez, V.; Sontag, R. L.; Moore, R. J.; Hu, D.; Mehta, H. S.; Cantlon-Bruce, J.; Liu, T.; Adkins, J. N.; Smith, R. D.; Clair, G. C.; Pasa-Tolic, L.; Zhu, Y., High-throughput and high-efficiency sample preparation for single-cell proteomics using a nested nanowell chip. *Nature Communications* **2021,** *12* (1), 6246.
19. Liang, Y.; Acor, H.; McCown, M. A.; Nwosu, A. J.; Boekweg, H.; Axtell, N. B.; Truong, T.; Cong, Y.; Payne, S. H.; Kelly, R. T., Fully Automated Sample Processing and Analysis Workflow for Low-Input Proteome Profiling. *Analytical Chemistry* **2021,** *93* (3), 1658-1666.
20. Sanchez-Avila, X.; Truong, T.; Xie, X.; Webber, K. G. I.; Johnston, S. M.; Lin, H.-J. L.; Axtell, N. B.; Puig-Sanvicens, V.; Kelly, R. T., Easy and Accessible Workflow for Label-Free Single-Cell Proteomics. *Journal of the American Society for Mass Spectrometry* **2023,** *34* (10), 2374-2380.
21. Gebreyesus, S. T.; Siyal, A. A.; Kitata, R. B.; Chen, E. S.-W.; Enkhbayar, B.; Angata, T.; Lin, K.-I.; Chen, Y.-J.; Tu, H.-L., Streamlined single-cell proteomics by an integrated microfluidic chip and data-independent acquisition mass spectrometry. *Nature Communications* **2022,** *13* (1), 37.
22. Wang, J.; Valentine, S. J.; Li, P., Integrated sample desalting, enrichment, and ionization on an omniphobic glass slide for direct mass spectrometry analysis. *Rapid Communications in Mass Spectrometry* **2021,** *35* (20), e9179.
23. Wang, J.; Curtin, K.; Valentine, S. J.; Li, P., Unlocking the potential of 3D printed microfluidics for mass spectrometry analysis using liquid infused surfaces. *Analytica Chimica Acta* **2023,** *1279*, 341792.
24. Yang, C.; Wu, L.; Li, G., Magnetically Responsive Superhydrophobic Surface: In Situ Reversible Switching of Water Droplet Wettability and Adhesion for Droplet Manipulation. ACS Applied Materials & Interfaces 2018, 10 (23), 20150-20158
25. Curtin, K.; Wang, J.; Fike, B. J.; Binkley, B.; Li, P., A 3D printed microfluidic device for scalable multiplexed CRISPR-cas12a biosensing. *Biomedical microdevices* **2023,** *25* (3), 34.
26. He, Z.; Huffman, J.; Curtin, K.; Garner, K. L.; Bowdridge, E. C.; Li, X.; Nurkiewicz, T. R.; Li, P., Composable Microfluidic Plates (cPlate): A Simple and Scalable Fluid Manipulation System for Multiplexed Enzyme-Linked Immunosorbent Assay (ELISA). Analytical Chemistry 2021, 93 (3), 1489-1497.
27. Zhu, Y.; Clair, G.; Chrisler, W. B.; Shen, Y.; Zhao, R.; Shukla, A. K.; Moore, R. J.; Misra, R. S.; Pryhuber, G. S.; Smith, R. D.; Ansong, C.; Kelly, R. T., Proteomic Analysis of Single Mammalian Cells Enabled by Microfluidic Nanodroplet Sample Preparation and Ultrasensitive NanoLC-MS. *Angewandte Chemie (International ed. in English)* **2018,** *57* (38), 12370-12374.
28. Dou, M.; Zhu, Y.; Liyu, A.; Liang, Y.; Chen, J.; Piehowski, P. D.; Xu, K.; Zhao, R.; Moore, R. J.; Atkinson, M. A.; Mathews, C. E.; Qian, W.-J.; Kelly, R. T., Nanowell-mediated two-dimensional liquid chromatography enables deep proteome profiling of <1000 mammalian cells. *Chemical Science* **2018,** *9* (34), 6944-6951.
29. Couvillion, S. P.; Zhu, Y.; Nagy, G.; Adkins, J. N.; Ansong, C.; Renslow, R. S.; Piehowski, P. D.; Ibrahim, Y. M.; Kelly, R. T.; Metz, T. O., New mass spectrometry technologies contributing towards comprehensive and high throughput omics analyses of single cells. *Analyst* **2019,** *144* (3), 794-807.